Chinese Journal of Natural Medicines

Five new meroterpenoids from *Rhododendron anthopogonoides* and their anti-inflammatory activity

Mengtian Li, Norbu Kelsang, Yongqin Zhao, Wensen Li, Feng Zhou, Pema , Lu Cui, Xianjie Bao, Qian Wang, Xin Feng, Minghua Yang

Citation: Mengtian Li, Norbu Kelsang, Yongqin Zhao, Wensen Li, Feng Zhou, Pema , Lu Cui, Xianjie Bao, Qian Wang, Xin Feng, Minghua Yang, Five new meroterpenoids from *Rhododendron anthopogonoides* and their anti-inflammatory activity, Chinese Journal of Natural Medicines, 2025, 23(7), 881-887. doi: 10.1016/S1875-5364(25)60850-8.

View online: https://doi.org/10.1016/S1875-5364(25)60850-8

Chinese Journal of Natural Medicines 23 (2025) 881-887

Contents lists available at ScienceDirect

Chinese Journal of Natural Medicines

journal homepage: www.cjnmcpu.com/

Original article

Five new meroterpenoids from *Rhododendron anthopogonoides* and their anti-inflammatory activity

Mengtian Li[a,Δ], Norbu Kelsang[b,c,Δ], Yongqin Zhao[a], Wensen Li[a], Feng Zhou[b,c], Pema[b,c], Lu Cui[d], Xianjie Bao[d], Qian Wang[e], Xin Feng[d,e,*], Minghua Yang[a,*]

[a] *State Key Laboratory of Natural Medicines, Jiangsu Key Laboratory of Bioactive Natural Product Research, School of Traditional Chinese Pharmacy, China Pharmaceutical University, Nanjing 210009, China*

[b] *Tibet Ganlu Pharmaceutical Technology Company, Lhasa 850032, China*

[c] *Technological Innovation Center of Traditional Tibetan Medicine Modernization of Tibet Autonomous Region, Lhasa 850032, China*

[d] *Beijing Hospital of Tibetan Medicine, China Tibetology Research Center, Beijing 100029, China*

[e] *Tibetan Medicine Institute, China Tibetology Research Center China, Beijing 100101, China*

ARTICLE INFO

Article history:
Received 23 August 2024
Revised 16 October 2024
Accepted 23 December 2024
Available online 20 July 2025

Keywords:
Anti-inflammatory
Tibetan medicine
Natural products
Isolation and identification
Rhododendron athopogonosides Maxim

ABSTRACT

Five meroterpenoids, rhodonoids K–M (**1**–**2**), daurichromene E (**3**), and grifolins A–B (**4**–**5**), together with seven known compounds (**6**–**12**), were isolated from *Rhododendron anthopogonoides*. The chemical structures of these compounds were elucidated through comprehensive analysis of high-resolution electrospray ionization mass spectrometry (HR-ESI-MS), ultraviolet (UV), infrared spectroscopy (IR), and nuclear magnetic resonance (NMR) data. Their absolute configurations were determined by comparing experimental electronic circular dichroism (ECD) spectra with computed values. Notably, compounds **1** and **3** demonstrated significant inhibitory effects on lipopolysaccharide (LPS)-induced inflammation in RAW264.7 cells. These compounds markedly suppressed the mRNA expressions of inflammatory factors, including interleukin (IL)-1β, IL-6, and tumor necrosis factor-α (TNF-α) while also down-regulating the protein expressions of inducible nitric oxide synthase (iNOS) and cyclooxygenase-2 (COX-2).

1. Introduction

Rhododendron athopogonosides Maxim., a perennial evergreen shrub, thrives in high-altitude regions across several provinces in China, including Sichuan, Gansu, Yunnan Provinces, and the Tibet Autonomous Region [1, 2]. It is a well-documented medicinal species in Tibetan ethnomedicine, where its flowers, leaves, and twigs are traditionally employed to treat disorders collectively referred to as “Peigen” in the Tibetan language [3], making *R. athopogonosides* a prevalent component in traditional Tibetan prescriptions. Phytochemical investigations have revealed that the extracts of *R. athopogonosides* exhibit various bioactivities, such as antioxidant [4], insecticidal [2], bacteriostatic [5], anti-inflammatory activities [6]. These biological properties have driven increasing interest in identifying its pharmacologically active constituents, which are primarily classified as flavonoids [7], essential oils [8], and triterpenes [9]. Among these, flavonoids and essential oils have been extensively studied andare recognized for their therapeutic relevance in respiratory and cardiovascular diseases [10].

Meroterpenoids, a structurally diverse class of natural products resulting from hybrid biosynthetic pathways, are typically categorized into polyketide-terpenoid and non-polyketide terpenoid subtypes [11] based on their biosynthetic origin. The genus *Rhododendron* has emerged as a prolific source of polyketide-derived meroterpenoids [12], especially those containing chromane or chromene scaffolds. This genus has yielded over one hundred meroterpenoids [13, 14] exhibiting diverse structural skeletons and biological activities. Although *R. athopogonosides* is known to produce meroterpenoids, systematic studies of this species remain relatively scarce. Iwata and Kitanaka [15], followed by Shi et al. [6], reported several structurally novel meroterpenoids from this plant, highlighting their significant anti-inflammatory potential. Driven by our continuing interest in bioactive meroterpenoids from medicinal plants [16, 17], we investigated the chemical composition of *R. athopogonosides* from Tibet. This work led to the isolation and structural characterization of five previously undescribed meroterpenoids (**1**–**5**) (Fig. 1), and seven known compounds (**6**–**12**). Among these, compounds **1** and **3** exhibited significant anti-inflammatory effects in lipopolysaccharide (LPS)-induced RAW264.7 cells. This study presents the isolation, structural elucidation, and anti-inflammatory activity of these compounds.

2. Results and discussion

Compound **1** was obtained as a yellow oil. Its molecular for-

* Corresponding author.
E-mail addresses: fengxin0303@163.com (X. Feng); skeepjack@163.com (M. Yang)
Δ These authors contributed equally to this work.

https://doi.org/10.1016/S1875-5364(25)60850-8

mula $C_{22}H_{30}O_3$ was established by the high-resolution electrospray ionization mass spectrometry (HR-ESI-MS) (*m/z* 365.2089 $[M + Na]^+$, Calcd. for $C_{22}H_{30}O_3Na$ 365.2087), indicating eight degrees of structural unsaturation. The ^1H nuclear magnetic resonance (NMR) spectrum (Table 1) showed two phenyl protons [δ_H 6.16 (s, H-6); 6.28 (s, H-8)], one olefinic proton [δ_H 5.46 (t, *J* = 5.4 Hz, H-15)], a pair of terminal olefinic protons [δ_H 4.80 (s, H-19a); 4.58 (s, H-19b)], and three methyls [δ_H 1.70 (s, H-18); 1.35 (s, H-20); 2.20 (s, H-21)]. Heteronuclear single quantum coherence (HSQC) correlations facilitated the identification of additional protons, including seven methylenes [δ_H 1.89 (m, *J* = 13.2, 3.0 Hz, H-3); 1.54 (m, H-9); 1.57 (m, H-10); 2.27 (m, H-13); 2.28 (m, H-14); 4.01 (s, H-17)] and three methines [δ_H 3.25 (m, H-4); 2.29 (m, H-11); 5.46 (t, H-15)]. The corresponding carbons were all found in the ^{13}C NMR spectrum (Table 1), which also included six non-proton-bearing olefinic ones and one quaternary carbon. These data were similar to those of rhodonoid G [18], a known meroterpenoid from *R. athopogonosides*.

The identical chromane core was confirmed by the similar chemical shifts of downfield-shifted C-2 and C-8a, along with the heteronuclear multiple bond correlations (HMBCs) (Fig. 2), especially from H-4 to C-2/C-3/C-8a, from H-6 to C-4a/C-5, from H-8 to C-4a/C-8a, from H_3-20 to C-2/C-3, and from H_3-21 to C-6/C-7/C-8. The correlations from H-9 to C-2/C-3/C-10/C-11, from H-4 to C-4a/C-5, and from H-20 to C-9 further established the same benzo[*c*]-2-oxabicyclo[3.3.1]nonane structure like rhodonoid G, which was also consistent with the observed spin system from C-3 to C-9 in ^1H–^1H correlation spectroscopy (COSY) spectrum (Fig. 2). The difference was found at the substitution of C-11 in **1**. Compound **1** exhibited a 2-methylhepta-2,6-dien-1-ol side chain, evidenced by the ^1H–^1H COSY correlations (Fig. 2) of H-13/H-14/H-15 and the HMBCs (Fig. 2) from H-18 to C-15/C-16/C-17, from H-15 to C-13/C-14/C-17, and from H-19 to C-11/C-12/C-13. It was settled at C-11 by the HMBCs (Fig. 2) from H-13 to C-11 and C-14. Thus, its planner structure was determined as shown. In the ROESY experiment (Fig. 3), the correlation between H-15 and H-17 indicated the *E*-orientation of C-15/C-16 double bond. The correlations from H-3a to H-4 and H_3-20 revealed their identical orientation. H-11, however, showed no useful correlations for configuration determination. The theoretical calculation of electronic circular dichroism (ECD) spectra was conducted to determine the configuration, which was based on time-dependent density functional theory (TD-DFT) at the B3LYP/6-31 + G(d, p) level. The two possible combinations of C-11 configuration were both submitted for calculation. The calculated ECD curves of 2*S*,4*S*,11*R* showed an excellent fit with the experimental one. Thus, the structure of compound **1** was determined as shown.

Compound **2**, a brown oil, was assigned a molecular formula of $C_{16}H_{20}O_3$ by HR-ESI-MS (*m/z* 261.1485 $[M + H]^+$, Calcd. for $C_{16}H_{21}O_3$ 261.1485), indicating seven degrees of unsaturation. The 1D NMR data of **2** resembled to those of **1** (Table 2), and the same benzo[*c*]-2-oxadicyclo[3.3.1]nonane ring system was further determined by the similar ^1H–^1H COSY and HMBCs (Fig. 2). The key structural difference was the presence of an acetyl group at C-11, as evidenced by HMBCs (Fig. 2) from methyl H-13 to C-11 and carbonyl C-12 and from H-10 and H-4 to C-12. In addition, rotating frame nuclear Overhauser effect spectroscopy (ROESY) revealed a consistent spatial orientation of H-4 and H_3-14, while the lack of correlation between H-4 and H-11 indicated an opposite orientation at C-11. ECD calculations (Fig. 4) confirmed the absolute configuration as 2*S*,4*S*,11*R* configuration for **2**.

Compound **3** was isolated as a brown oil with molecular formula $C_{22}H_{32}O_4$ determined by the HR-ESI-MS (*m/z* 383.2192 $[M + Na]^+$, Calcd. for $C_{22}H_{32}O_4Na$ 383.2193). The NMR data of **3** showed high similarity with daurichromene D [19], a prenylated orcinol derivative isolated from *R. dauricum*. However, compound **3** exhibited one additional oxygen and two additional hydrogen atoms, indicating that **3** is an additional product of daurichromene D [19]. This inference was corroborated by the absence of C-3/C-4 double bond signals and the presence of an oxygen-bearing methenyl at δ_C 68.3. Further evidence was provided by the ^1H–^1H COSY correlations (Fig. 2) between H-3 and H-4, and the HMBCs (Fig. 2) from H-4 to C-2, C-3, C-4a, C-8a and C-5, and from H-3 to C-20. The comprehensive analysis of 2D NMR data further determined the planar structure of **3**. In ROESY spectrum (Fig. 3), the correlations of H-11/H-13 and H-15/H-17 established the *E*-orientation of double bonds in the side chain. The correlation of H-3/H-20 indicated their same orientation. To elucidate the absolute configuration, time-dependent density functional theory calculations of ECD spectra were performed (Fig. 4). The experimental spectrum closely aligned with the calculated one for the 2*R*,3*R* configurations. Thus, **3** was determined as shown.

Compound **4**, obtained as a brown oil, had a molecular formula of $C_{22}H_{32}O_3$ based on HR-ESI-MS ion at *m/z* 367.2244 $[M + Na]^+$ (Calcd. for $C_{22}H_{32}O_3Na$ 367.2244). Its ^1H NMR spectrum (Table 3) showed signals for two *meta*-coupled aromatic protons [δ_H 6.22 (s, H-4); 6.22 (s, H-6)], three olefinic protons [δ_H 5.25 (t, *J* = 6.5 Hz, H-8); 5.07 (t, *J* = 6.5 Hz, H-12); 5.38 (t, *J* = 6.5 Hz, H-16)], and four methyls [δ_H 2.18 (s, H-22); 1.66 (s, H-19); 1.58 (s, H-20); 1.80 (s, H-21)]. The corresponding carbons were also found in ^{13}C

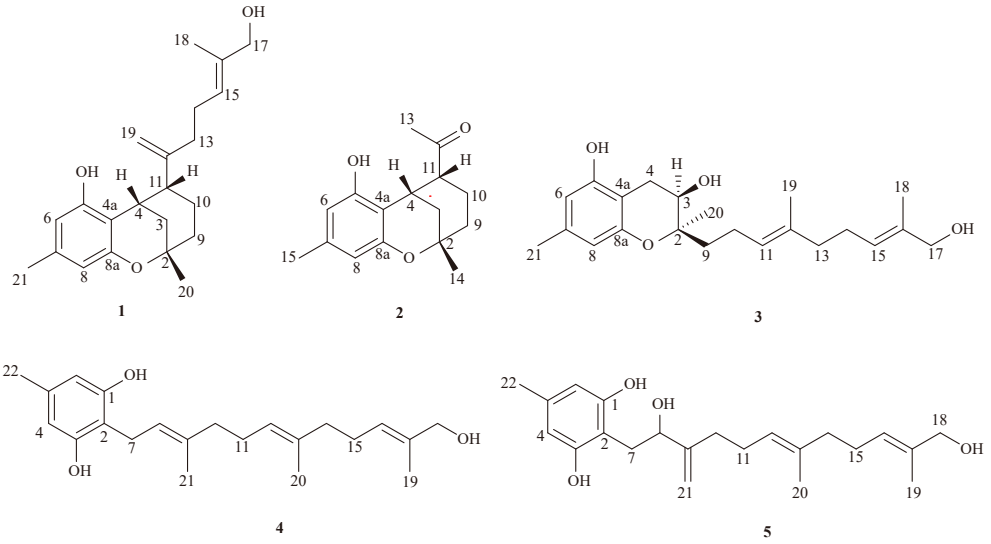

Fig. 1 Structures of compounds **1**–**5**.

Table 1 The ^{1}H (600 MHz) and ^{13}C (150 MHz) NMR data for **1** and **2** (J in Hz).

No.	**1**[a]		**2**[b]	
	δ_H (J in Hz)	δ_C	δ_H (J in Hz)	δ_C
2		73.8		74.6
3	1.89, dd (13.2, 3.0) 1.79, dt (13.2, 3.0)	37.6	2.00, dd (13.2, 3.0) 1.76, dt (12.6, 3.0)	38.0
4	3.25, m	32.2	3.74, br s	30.7
4a		107.8		107.4
5		153.4		155.9
6	6.16, s	108.3	6.04, s	107.4
7		137.5		138.8
8	6.28, s	109.0	6.09, s	108.2
8a		157.2		158.6
9	1.54, m 2.01, m	39.8	1.93, dt (9.0, 2.4) 1.56, m	39.6
10	1.57, m 1.42, m	23.5	1.57, m 1.41, m	20.9
11	2.29, m	47.6	2.83, m	56.1
12		152.0		213.6
13	2.27, m 2.17, m	35.7	2.28, s	29.1
14	2.28, m	25.0	1.33, s	29.2
15	5.46, t (5.4)	125.4	2.15, s	21.4
16		135.8		
17	4.01, s	68.8		
18	1.70, s	13.9		
19	4.58, s 4.80, s	110.0		
20	1.35, s	28.8		
21	2.20, s	21.4		

[a] in $CDCl_3$; [b] in CD_3OD.

NMR. Additionally, HSQC correlations indicated the presence of six methylenes. These 1D NMR data were comparable to those of grifolin [20], while the presence of a downfield-shifted methylene (δ_C 69.1) revealed an oxidative methyl in **4**. The singlet methylene at δ_H 4.00 showed HMBCs with C-16 and C-19 (Fig. 2), confirming the hydroxyl substitution at C-18. Furthermore, ROESY correlations from H-8 to H-10, from H-12 to H-14, and from H-16 to H-18 indicated the *trans*-configuration of the three double bonds (Fig. 3).

Compound **5**, also a brown oil, had a molecular formula of $C_{22}H_{32}O_4$ (*m/z* 383.2193 $[M + Na]^+$, Calcd. 383.2193), indicating an additional oxygen atom compared to **4**. Structural elucidation using 2D NMR revealed that **5** is an oxidized derivative of **4**. Key HMBCs from terminal olefinic protons [δ_H 4.88 (m, H-21a); 5.10 (d, J = 7.0 Hz, H-21b)] (Fig. 2) to C-8, C-9, and C-10 were detected, and the methine proton at C-8 [δ_H 4.31 (d, J = 6.5 Hz, H-8)] displayed $^{1}H-^{1}H$ COSY correlation (Fig. 2) with H-7 and critical HMBCs (Fig. 2) with C-2, C-7, C-10, and C-21. Additional 2D NMR data (Fig. 2) further confirmed the structure of **5**. The near-zero optical rotation and flat ECD curve suggested a racemic or nearly racemic mixture, which was validated by chiral high-performance liquid chromatography (HPLC), revealing two enantiomeric peaks in approximately equal proportions.

The remaining known compounds were identified as loliolide (**6**) [21], caffeic acid methyl ester (**7**) [22], chlospicate C (**8**) [23], istanbulin A (**9**) [24], 4α-hydroxy-5α,8β(*H*)-eduesm-7(11)-en-8,12-olidel (**10**) [25], chlospicate D (**11**) [23], and 6(1*H*)-azulenone (**12**) [26] by comparing their NMR data with those reported in literature.

All compounds were evaluated for cytotoxicity and anti-inflammatory activity in LPS-induced RAW264.7 macrophages. The CCK-8 assay confirmed that all tested compounds were non-toxic at concentrations up to 50 μmol·L^{-1}. The compounds were then tested for their inhibitory effects on NO production, with L-NMMA (IC_{50} 40.58 ± 0.86 μmol·L^{-1}) as the positive control. Most compounds showed weak or no inhibition (IC_{50} 50 μmol·L^{-1}), whereas compounds **1** and **3** displayed moderate NO inhibition with IC_{50} values of 10.75 ± 2.28 and 15.85 ± 1.58 mol·L^{-1}, respectively. To explore their mechanism of action, the effects of compounds **1** and **3** on the mRNA expression of key inflammatory markers—tumor necrosis factor-α (*TNF-α*), interleukin *(IL)-1β*, *IL-6*, cyclooxygenase-2 (*COX-2*), and inducible nitric oxide synthase (*iNOS*) —were assessed by quantitative reverse transcription-polymerase chain reaction (qRT-PCR). As shown in Figs. 5A–5E, Both compounds significantly suppressed these markers in a dose-dependent manner. They both showed a good inhibition rate of *IL-1β* since about 50% mRNA expression was inhibited at the concentration of 12.5 μmol·L^{-1}. Compound **1** exhibited stronger suppression of *COX-2* mRNA (34.5% ± 3.22% inhibition), while compound **3** more effectively reduced *iNOS* expression. Western blotting analysis confirmed these effects at the protein level (Figs. 5F–5K): compound **1** preferentially downregulated COX-2, while **3** was more effectively suppressed iNOS expression, suggesting divergent but complementary anti-inflammatory mechanisms.

3. Conclusion

In this study, five previously undescribed meroterpenoids, rhodonoids K and M (**1** and **2**), daurichromene E (**3**), and grifolins A and B (**4** and **5**), were isolated and structurally elucidated from *R. anthopogonoides*. Their structures and absolute configurations were determined through comprehensive spectroscopic analysis. Compounds **1** and **3** exhibited moderate but significant anti-inflammatory activity in LPS-stimulated RAW264.7 macrophages, demonstrated by their ability to reduce nitric oxide production and downregulate the expression of key inflammatory mediators at both mRNA and protein levels. Thus, these meroterpenoids are considered to be the bioactive constituents responsible for the anti-inflammatory properties of *R. anthopogonoides*.

4. Experimental

4.1. Materials and methods

ECD spectra were obtained using a Jasco J-810 Circular dichroism spectrometer (JASCO, Japan). Ultraviolet (UV) spectra were obtained using a UV-2450 spectrophotometer (Shimadzu, Japan). IR spectra were measured using a Bruker Tensor-27 spectrophotometer (Bruker, Germany). Optical rotations were measured on a Jasco P-1020 polarimeter (JASCO, Japan). NMR spectra were recorded on a Bruker Avance III-500 or Bruker Avance III-600 spectrometer (Bruker, Germany) with TMS as an internal standard. HR-ESI-MS data were recorded on Micro Q-TOF MS spectrometer (Waters, USA). ESI-MS data were recorded on Agilent 1100 (Agilent, USA). Column chromatography was performed on silica gel (200–300 mesh, 100–200 mesh, Qingdao

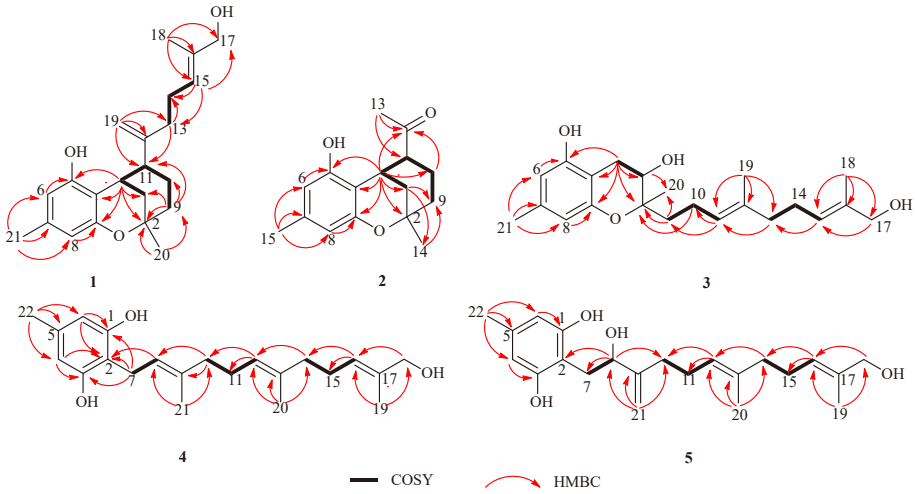

Fig. 2 Key $^{1}H-^{1}H$ COSY and HMBCs of compounds **1–5**.

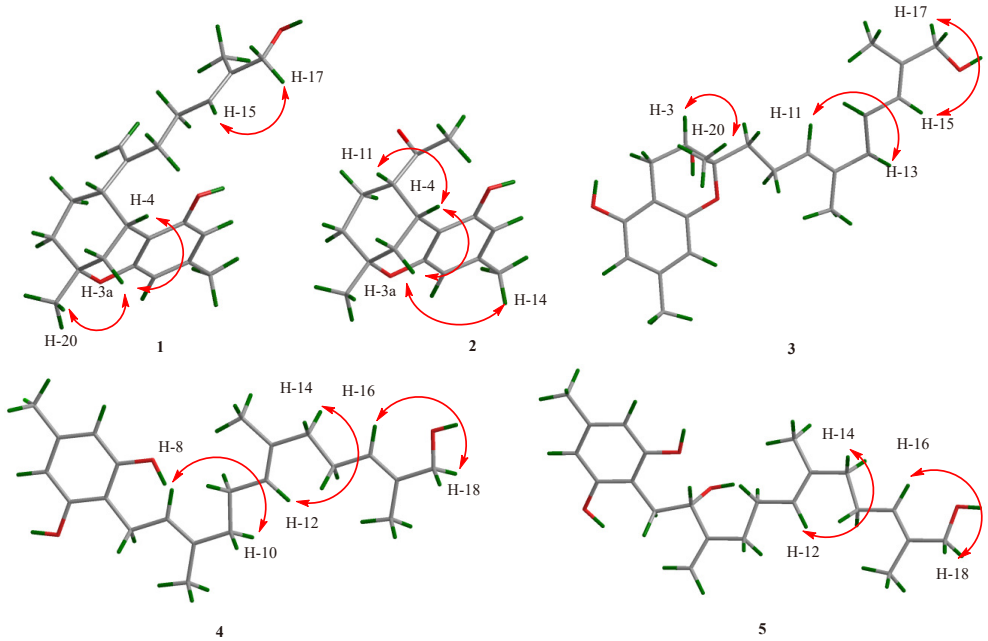

Fig. 3 Key ROSEY correlations of compounds **1–5**.

Table 2 The ^{1}H (600 MHz) and ^{13}C (125 MHz) NMR data for **3** in $CDCl_3$ (*J* in Hz).

No.	δ_H	δ_C	No.	δ_H	δ_C
2		78.4	11	5.12, t (6.0)	122.4
3	3.87, t (4.5)	68.3	12		132.7
4	2.62, dd (14.0, 5.0) 2.87, dd (14.0, 5.0)	28.3	13	2.02, t (6.0)	41.1
			14	2.12, m	28.3
4a		102.6	15	5.34, t (5.0)	123.5
5		150.0	16		132.3
6	6.19, s	106.5	17	3.98, s	69.4
7		135.1	18	1.64, s	16.8
8	6.27, s	108.6	19	1.59, s	18.9
8a		150.8	20	1.28, s	22.0
9	1.64, m	39.0	21	2.20, s	24.0
10	2.12, m	24.4			

Marine Chemical Inc., Qingdao, China), MCI gel CHP20/P120 (37–73 μm, Mitsubishi Chemical Industries, Tokyo, Japan), RP-18 (40–63 μm, Fuji Silysia Chemical Ltd., Tokyo, Japan), and Sephadex LH-20 (Amersham Pharmacia, Uppsala, Sweden). Preparative HPLC was carried out by using a Shimadzu LC-8A chromatograph equipped with a Shim-pack ODS (250 mm × 20 mm, 5 μm). Analytical HPLC was performed using an Agilent 1260 chromatograph equipped with a Shim-pack ODS (4.6 mm × 250 mm, 5 μm).

4.2. Plant material

R. anthopogonoides specimens were collected from Tibet, China in August 2021. The plant material was taxonomically identified by Prof. Chaofeng Zhang of China Pharmaceutical University. The voucher specimen (No. 2022-LXDJ) was deposited at the Herbarium of the Department of Chemistry, China Pharmaceutical University (China).

4.3. Extraction and isolation

Dried and powdered aerial parts of *R. anthopogonoides* (1 kg)

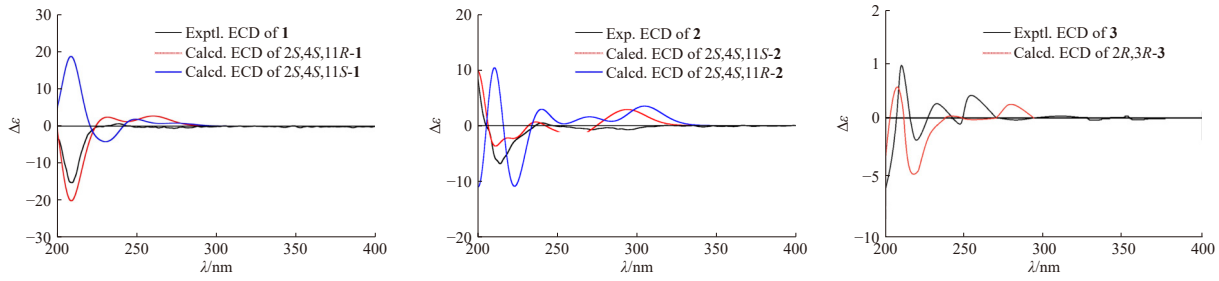

Fig. 4 Experimental and calculated ECD of compounds **1**–**3**.

Table 3 The ^{1}H (600 MHz) and ^{13}C (125 MHz) NMR data for **4** and **5** in $CDCl_3$ (*J* in Hz)

No.	**4**		**5**	
	δ_H (*J* in Hz)	δ_C	δ_H (*J* in Hz)	δ_C
1		155.0		155.7
2		110.8		110.4
3		155.0		155.7
4	6.22, s	109.0	6.26, s	109.4
5		137.4		138.0
6	6.22, s	109.0	6.26, s	109.4
7	3.38, d (6.5)	22.3	2.73, dd (12.0, 7.5) 3.09, d (12.0)	29.8
8	5.25, t (6.5)	122.2	4.31, d (6.5)	77.0
9		138.2		151.4
10	2.03, m	39.7	2.20, m	26.1
11	2.06, m	26.2	2.19, m	32.2
12	5.07, t (6.5)	126.7	5.13, m	124.7
13		135.1		134.8
14	2.07, m	39.2	2.05, m	39.0
15	2.08, m	26.0	2.14, m	25.5
16	5.38, t (6.5)	126.7	5.33, m	125.7
17		134.3		134.3
18	4.00, s	69.1	3.98, s	68.8
19	1.66, s	13.8	1.63, s	13.9
20	1.58, s	16.1	1.60, s	16.1
21	1.80, s	16.3	4.88, m 5.10, d (7.0)	108.9
22	2.18, s	21.2	2.20, s	21.3

were refluxed with 95% EtOH (3 × 5 L, 3 h each). The combined extracts were concentrated under reduced pressure to yield approximately 100 g of residue, which was then suspended in water and partitioned thrice with petroleum ether (PE) and ethyl acetate (EtOAc) sequentially. The PE fraction (20 g) was subjected to silica gel column chromatography (elution with PE/EtOAc, gradient from 1∶0 to 1∶2, *V*/*V*), yielding five fractions (Frs. 1–5). Fr. 3 (2.5 g) was further purified using a Sephadex LH-20 column eluted with methanol (MeOH)/dichloromethane (CH_2Cl_2) (1∶1, *V*/*V*), yielding 8 subfractions (Frs. 3.1–3.8). Fr. 3.2 (210.8 mg) was then subjected to preparative HPLC (MeOH–H_2O, 40∶60, *V*/*V*) to yield compounds **1** (6.4 mg, t_R 37.5 min) and **2** (9.2 mg, t_R 42.6 min). Fr. 5 (3.5 g) was subjected to an ODS column eluted with MeOH/H_2O (35∶65→100∶0, *V*/*V*) to obtain 12 subfractions (Frs. 5.1–5.12). Fr. 5.2 (202.4 mg) was further purified by preparative HPLC (MeOH–H_2O, 60∶40, *V*/*V*) to yield compound **3** (10.1 mg, t_R 29.4 min). Fr. 5.4 (222.8 mg) was also purified by preparative HPLC (MeOH–H_2O, 50∶50, *V*/*V*) to obtain compounds **4** (11.0 mg, t_R 38.4 min) and **5** (8.6 mg, t_R 40.2 min). The EtOH part (40 g) was separated using a silica gel column and eluted with CH_2Cl_2/MeOH (1∶0→1∶2, *V*/*V*) to yield 8 fractions (Frs. 6–13). Fr. 8 (4.0 g) was further purified using an ODS column eluted with MeOH/H_2O (35∶65→100∶0, *V*/*V*), yielding 14 subfractions (Frs. 8.1–8.14). Fr. 8.2 (120.5 mg) was finally purified by preparative HPLC (MeOH–H_2O, 45∶55, *V*/*V*) to obtain compound **6** (20.4 mg, t_R 20.4 min). Compounds **7** (15.6 mg, t_R 21.0 min) and **8** (9.5 mg, t_R 24.3 min) were isolated from Fr. 8.5 using preparative HPLC (MeOH–H_2O, 45∶55, *V*/*V*). Fr. 8.4 was finally purified by preparative HPLC (MeOH–H_2O, 45∶55, *V*/*V*) to obtain compound **9** (8.7 mg, t_R 30.6 min). Fr. 8.5 placed steadily to precipitate compound **10** (16.8 mg). And finally, Fr. 8.6 was purified by preparative HPLC (MeOH–H_2O, 50∶50, *V*/*V*) to obtain compounds **11** (11.3 mg, t_R 37.5 min) and **12** (9.3 mg, t_R 38.2 min).

Rhodonoid K: yellow oil; $[\alpha]_D^{25}$ +16.0 (*c* 0.1, MeOH); UV (MeOH) λ_{max} (log ε) 282 (3.03), 274 (3.04), 208 (4.15), 193 (3.58) nm; IR (KBr) ν_{max} 3333, 2930, 1625, 1586, 1451, 1383, 1160, 1134, 1094, 997, 883 cm^{-1}; ^{1}H and ^{13}C NMR data (Table 1); HR-ESI-MS *m*/*z* 365.2089 [M + Na]$^+$ (Calcd. for $C_{22}H_{30}O_3Na$, 365.2087).

Rhodonoid L: brown oil; $[\alpha]_D^{25}$ −20.8 (*c* 0.1, MeOH); UV (MeOH) λ_{max} (log ε) 274 (3.09), 207 (3.96), 193 (3.48) nm; IR (KBr) ν_{max} 3269, 2931, 1686, 1624, 1588, 1451, 1347, 1159, 1097, 997, 823 cm^{-1}; ^{1}H and ^{13}C NMR data (Table 1); HR-ESI-MS *m*/*z* 261.1485 [M + H]$^+$ (Calcd. for $C_{16}H_{21}O_3$, 261.1485).

Daurichromene E: brown oil; $[\alpha]_D^{25}$ −9.6 (*c* 0.1, MeOH); UV (MeOH) λ_{max} (log ε) 280 (2.87), 273 (2.89), 207 (4.16) nm; IR (KBr) ν_{max} 3374, 2922, 1628, 1589, 1518, 1452, 1383, 1208, 1073, 996, 823, 574 cm^{-1}; ^{1}H and ^{13}C NMR data (Table 2); HR-ESI-MS *m*/*z* 383.2192 [M + Na]$^+$ (Calcd. for $C_{22}H_{32}O_4Na$, 383.2193).

Grifolin A: brown oil; UV (MeOH) λ_{max} (log ε) 276 (2.73), 207 (4.13) nm; IR (KBr) ν_{max} 3404, 2922, 1715, 1629, 1597, 1451, 1385, 1222, 1049, 989, 824, 591 cm^{-1}; ^{1}H and ^{13}C NMR data (Table 3); HR-ESI-MS *m*/*z* 367.2242 [M + Na]$^+$ (Calcd. for $C_{22}H_{32}O_3Na$, 367.2244).

Grifolin B: brown oil; $[\alpha]_D^{25}$ −1.4 (*c* 0.1, MeOH); UV (MeOH) λ_{max} (log ε) 276 (2.88), 207 (4.23) nm; IR (KBr) ν_{max} 3343, 2923, 1716, 1633, 1591, 1451, 1386, 1210, 1073, 903, 826, 590 cm^{-1}; ^{1}H and ^{13}C NMR data (Table 3; HR-ESI-MS *m*/*z* 367.2242 [M + Na]$^+$ (Calcd. for $C_{22}H_{32}O_3Na$, 367.2244).

4.4. Cell culture and viability assay

RAW264.7 cells were cultured in high-glucose DMEM supplemented with 10% FBS and 1% penicillin–streptomycin antibiotics in the atmosphere with 5% CO_2 at 37 °C. The isolated compounds were dissolved in DMSO for activity texting. Cell viability was assessment by cell counting kit-8 (CCK-8) assay. The cells (5 × 10^3 cells/well) was cultured in 96-well plates for 12 h, fol-

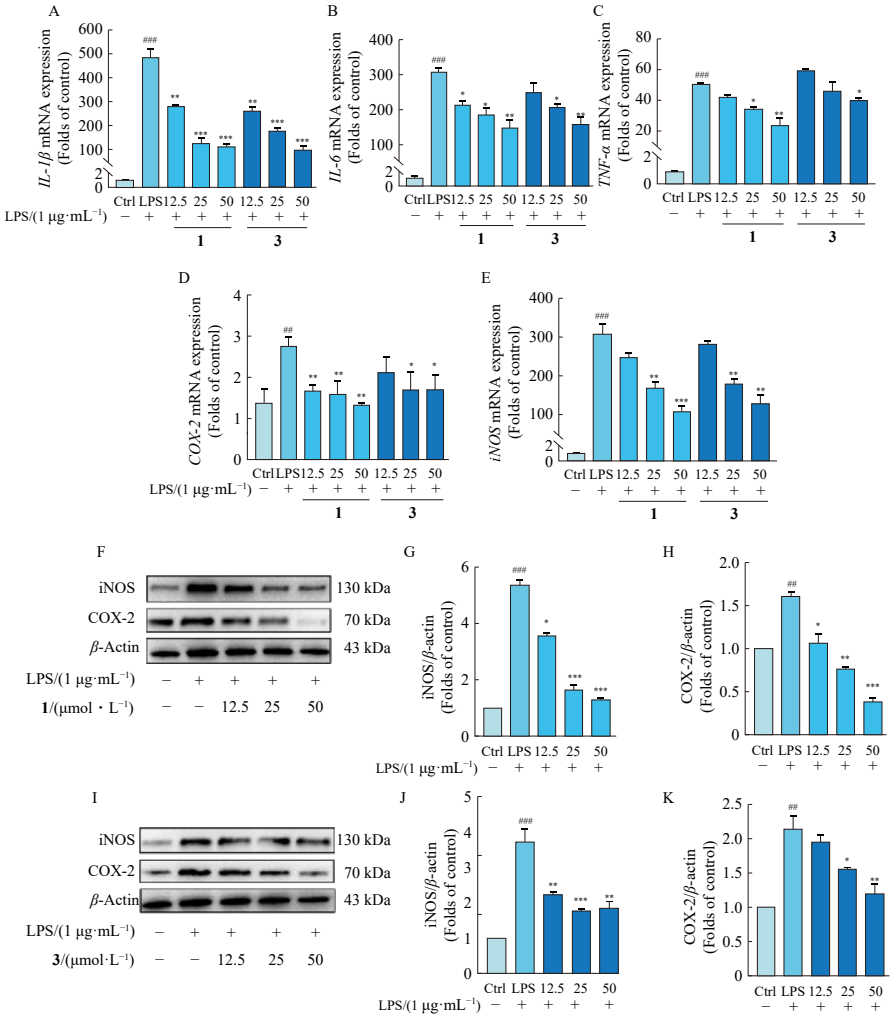

Fig. 5 Effects of compounds **1** and **3** on LPS-induced mRNA expression of *IL-1β* (A), *IL-6* (B), *TNF-α* (C), *COX-2* (D), and *iNOS* (E) in RAW264.7 cells were determined by qRT-PCR. Effects of compounds **1** (F–H) and **3** (I–K) on LPS-induced protein expression of COX-2 and iNOS in RAW264.7 cells were determined by Western blotting. Data are presented as mean ± SD (n = 3). $^{\#}P < 0.05$, $^{\#\#}P < 0.01$ and $^{\#\#\#}P < 0.001$ *vs* control group, $^{*}P < 0.05$, $^{**}P < 0.01$ and $^{***}P < 0.001$ *vs* LPS group.

lowed by treatment with the tested compounds **1**–**12** separately at different concentrations (0, 6.25, 12.5, 25, 50, 100 μmol·L^{-1}) for 24 h. After incubation with CCK-8 reagent (20 μL) for 1 h, the absorbance at 450 nm was measured with a microplate reader (TECAN, Switzerland).

4.5. NO production assay

NO levels in the culture supernatant were quantified using the Griess reagent nitrite measurement kit (Beyotime, China). RAW264.7 cells (2 × 10^5 cells/well) were cultured in 100 μL DMEM in 96-well plates for 12 h and then treated with different concentrations (0, 6.25, 12.5, 25, 50 μmol·L^{-1}) of compounds **1**–**5** for an additional 12 h. Lipopolysaccharide (LPS) at 1 μg·mL^{-1} was added as an inducer and cultured together with the compounds. After incubation, 50 μL of the supernatant was mixed with an equal volume of Griess reagent A and B. Following a 10-min shaking period, the absorbance was measured at 450 nm using a microplate reader (TECAN, Switzerland), and subsequently, the NO inhibition rates were calculated.

4.6. Quantitative real-time PCR analysis

Total RNA was isolated using a total RNA isolation kit (Vazyme, China), and RNA concentration was measured using a NanoDrop One Spectrophotometer (Thermo, USA). First-strand cDNA was synthesized from total RNA and used for qRT-PCR using SYBR Green Master Mix (Vazyme, China) on a Roche LightCycler system. Expression levels of *TNF-α*, *IL-1β*, *IL-6*, *COX-2*, and *iNOS* were quantitatively analyzed using the Real-Time PCR Detection System (Roche, Switzerland). The quantitative primers employed for amplification are listed in Supplementary Table 1.

4.7. Western blotting analysis

RAW264.7 cells (1 × 10^5 cells/well) were cultured in 6-well plates for 12 h and pretreated with compounds **1** or **3** at gradient concentrations for 12 h, followed by co-stimulation with 1 μg·mL^{-1} LPS. Total protein was extracted and quantified using a bicinchoninic acid (BCA) assay. Equal amounts of protein were separated by sodium dodecyl sulfate-polyacrylamide gel electrophoresis (SDS-PAGE) and transferred onto the immunoblot membranes. Protein bands were detected using an enzyme marker. Membranes were blocked and incubated overnight at 4 °C with primary antibodies against COX-2, iNOS, or *β*-actin. After washing with tris-buffered saline with Tween 20 (TBST), membranes were incubated with secondary antibodies at room temperature for 1 h. Finally, the membranes were visualized using a Gel Documentation System.

Funding

This work was supported by the second batch of Bureau-level Projects of the Tibetan Medicine Administration of the Tibet

Autonomous Region in 2020 (No. JJKT20200024).

Availability of supporting information

Supporting information for this study can be obtained by contacting the corresponding authors *via* E-mail.

Declaration of competing interest

These authors have no conflict of interest to declare.

References

1 Committee of Flora of China. *Flora of China*. Beijing: Science Press. 1990:180.
2 Yang K, Zhou YX, Cheng FW, et al. Toxicity of *Rhododendron anthopogonoides* essential oil and its constituent compounds towards *Sitophilus zeamais*. *Molecules*. 2011;16(9):7320-7330. https://doi.org/10.3390/molecules16097320.
3 Demar DP. *JinDru Bencao*. Shanghai Scientific & Technical Publishers. 2012: 68.
4 Jing LL, Ma HP, Fan PC, et al. Antioxidant potential, total phenolic and total flavonoid contents of *Rhododendron anthopogonoides* and its protective effect on hypoxia-induced injury in PC12 cells. *BMC Complem Altern Med*. 2015;15:1-12. https://doi.org/10.1186/s12906-015-0520-z.
5 Liang JY, Yang Q, Ma XM, et al. The content and antibacterial activity of volatile oil from three species of *Rhododendron* in Gansu Province. *Chin Wild Plant Resour*. 2014;33(4):9-10. https://doi.org/10.3969/j. issn.1006-9690.2014.04.003.
6 Shi Q, Li TT, Wu YM, et al. Meroterpenoids with diverse structures and anti-inflammatory activities from *Rhododendron anthopogonoides*. *Phytochemistry*. 2020;180:112524. https://doi.org/10.1016/j.phytochem.2020.112524.
7 Zhao L, Ge J, Qiao CD, et al. Separation and quantification of flavonoid compounds in *Rhododendron anthopogonoides* Maxim by high-performance liquid chromatography. *Acta Chromatogr*. 2008;20(1):135-146. https://doi.org/10.1556/AChrom.20.2008.1.11.
8 Guleria S, Jaitak V, Saini R, et al. Comparative studies of volatile oil composition of *Rhododendron anthopogon* by hydrodistillation, supercritical carbon dioxide extraction and head space analysis. *Nat Prod Res*. 2011; 25(13):1271-1277. https://doi.org/10.1080/14786419.2011.576395.
9 Dai SJ, Yu DQ. Triterpenoids of *Rhododendron anthopogonoides*. *Chin J Nat Med*. 2005;3(6):347-349.
10 Li XF, Jin HZ, Chen G, et al. Study advances on chemical constituents and pharmacological activities of the Tibetan medicine Dali. *Nat Prod Res Dev*. 2008;20:1125-1128. https://doi.org/10.16333/j.1001-6880.2008.06.019.
11 Nazir M, Saleem M, Tousif MI, et al. Meroterpenoids: a comprehensive update insight on structural diversity and biology. *Biomolecules*. 2021;11(7): 957. https://doi.org/10.3390/biom11070957.
12 Huang GH, Zhu LC, Wang PP, et al. Enantiomeric pairs of meroterpenoids with diverse heterocyclic systems from *Rhododendron nyingchiense*. *J Nat Prod*. 2018;81(8):1810-1818. https://doi.org/10.1021/acs.jnatprod.8b00273.
13 Liu XJ, Su HG, Peng XR, et al. An updated review of the genus *Rhododendron* since 2010: traditional uses, phytochemistry, and pharmacology. *Phytochemistry*. 2024;217:113899. https://doi.org/10.1016/j.phytochem.2023.113899.
14 Fuloria NK, Raheja RK, Shah KH, et al. Biological activities of meroterpenoids isolated from different sources. *Front Pharmacol*. 2022;13:830103. https://doi.org/10.3389/fphar.2022.830103.
15 Iwata N, Kitanaka S. New cannabinoid-like chromane and chromene derivatives from *Rhododendron anthopogonoides*. *Chem Pharm Bull*. 2011;59 (11):1409-1412. https://doi.org/10.1248/cpb.59.1409.
16 Shang ZC, Yang MH, Jian KL, et al. ^{1}H NMR-guided isolation of formyl-phloroglucinol meroterpenoids from the leaves of *Eucalyptus robusta*. *Chem Eur J*. 2016;22(33):11778-11784. https://doi.org/10.1002/chem.201601732.
17 Shang ZC, Han C, Xu JL, et al. Twelve formyl phloroglucinol meroterpenoids from the leaves of *Eucalyptus robusta*. *Phytochemistry*. 2019;163:111-117. https://doi.org/10.1016/j.phytochem.2019.04.008.
18 Liao HB, Huang GH, Yu MH, et al. Five pairs of meroterpenoid enantiomers from *Rhododendron capitatum*. *J Org Chem*. 2017;82(3):1632-1637. https://doi.org/10.1021/acs.joc.6b02800.
19 Iwata N, Wang N, Yao X, et al. Structures and histamine release inhibitory effects of prenylated orcinol derivatives from *Rhododendron dauricum*. *J Nat Prod*. 2004;67(7):1106. https://doi.org/10.1021/np0303916.
20 Mahiou V, Roblot F, Hocquemiller R, et al. Piperogalin, a new prenylated diphenol from *Peperomia galioides*. *J Nat Prod*. 1995;58(2):324-328. https://doi.org/10.1021/np50116a031.
21 Willuhn G, Westhaus RG. Loliolide (calendin) from *Calendula officinalis*. *Planta Med*. 1987;53(3):304. https://doi.org/10.1055/s-2006-962718.
22 Jouogo DCN, Eckhardt P, Tamokou J, et al. A new phenolic glycoside from the leaves of *Flacourtia flavescens* Willd. *Nat Prod Res*. 2024;3816:2737-2747. https://doi.org/10.1080/14786419.2023.2232078.
23 Yang SP, Chen HD, Yue JM. Sesquiterpenoids from *Chloranthus spicatus*. *Chin J Chem*. 2012;30:6. https://doi.org/10.1002/cjoc.201200455.
24 Buděínsky M, Holub M, Saman D, et al. Structure of istanbulin A and istanbulin B, two sesquiterpenic lactones from *Smyrnium olusatrum* L.. *Collect Czechoslov Chem Commun*. 1984;49(5):1311-1317. https://doi.org/10.1135/cccc19841311.
25 Xiao Z, Wang X, Zhang G, et al. Terpenoids from roots of *Chloranthus spicatus*. *Helv Chim Acta*. 2010;93(4):803-810. https://doi.org/10.1002/hlca.200900299.
26 Ohshiro M, Kuroyanagi M, Ueno A. Structures of sesquiterpenes from *Curcuma longa*. *Phytochemistry*. 1990;29(7):2201-2205. https://doi.org/10.1016/0031-9422(90)83038-3.